

A Two-Atom Picture of Coherent Atom-Molecule Quantum Beats

Bogdan Borca[†], D. Blume[‡], Chris H. Greene[†]

[†] JILA and Department of Physics, University of Colorado, Boulder, Colorado 80309-0440

[‡] Department of Physics, Washington State University, Pullman, Washington 99164-2814

E-mail: borca@jila.u1.colorado.edu

E-mail: doerte@wsu.edu

E-mail: Chris.Greene@Colorado.edu

Abstract. A simple two-atom model is shown to describe a Bose-Einstein condensate of alkali atoms subjected to external magnetic field ramps near a Feshbach resonance. The implications uncovered for two atoms in a trap can be applied at least approximately to a many-atom condensate. A connection to observations is accomplished by scaling the trap frequency to achieve a density comparable to that of the experiments, which yields the fraction of atom pairs in the gas that become molecules. A sudden approximation is used to model the external magnetic field ramps in the vicinity of a two-body Feshbach resonance. The results of this model are compared with recent experimental observations of Donley *et al.* [1].

PACS numbers: 03.75.Mn

Submitted to: *New J. Phys.*

1. Introduction

Utilizing Feshbach resonance physics, recent experiments have produced an atomic Bose-Einstein condensate (BEC) coherently coupled to molecules in high vibrationally excited bound states [1]. The coupling of atomic and molecular states was achieved through application of a pulsed external magnetic field and it has sparked much interest [2] since it ultimately (although possibly not yet) should lead to the creation of a molecular condensate. The problem of creating a molecular BEC has been one of the focus areas of ultracold physics research for several years now [3]. Two different techniques, namely photoassociation and a magnetic field ramp near a Feshbach resonance, have been used in attempts to transform an atomic condensate into a molecular one. The use of Feshbach resonances to control the atom-atom scattering length, and other properties, has been previously demonstrated experimentally [4, 5].

It was predicted theoretically [6] that magnetic field pulses would drive a significant part of an atomic BEC into a molecular one. These predictions were based on a mean field theory approach, of the same type that has proven very successful in describing many properties of the alkali atom BECs produced experimentally to date. However, two sets of experiments performed at JILA have shown puzzling results that did not match the original theoretical predictions. In one experiment, a single magnetic pulse close to the Feshbach resonance probed the strongly interacting atomic dynamics, [7] while in a second experiment double pulses generated interference patterns between the different states populated. In both experiments, the atoms, part of the initial BEC cloud, were observed to end up in one of the following three components: a remnant BEC cloud, a burst of hot atoms, and a missing (undetected) component. This outcome differed from the theoretical predictions which only accounted directly for two components. The questions regarding the nature of the three components observed experimentally, including the specific issue of whether a molecular BEC was created, were addressed by two independent theoretical papers [8, 9]. Both of these papers accounted for many body effects by employing field theory beyond the mean field (i.e., Gross-Pitaevskii equation) level. These two studies gave similar answers, in identifying the observed atom bursts as hot, non-condensed atoms, and the missing component as a molecular condensate. In addition to Refs. [8] and [9], three other theoretical studies involving many-body approaches have also addressed the interpretation of the Donley *et al.* experiment [10, 11, 12].

In this paper we propose an alternative model that does not rely on field theory. Our model considers only two-body dynamics and uses a very simple scaling procedure to apply our results to the many-body system studied experimentally. The observed oscillatory behavior can then be viewed as a simple example of quantum beats of the type that arise whenever indistinguishable quantum mechanical pathways associated with two or more impulsively-excited stationary states interfere coherently.[13] Specifically, our treatment considers two atoms confined by a spherically symmetric harmonic oscillator potential, which interact through a contact potential. The stationary states of such a

system have been described by Busch *et al.*, [14] who proposed it as a model that can be used in the context of ultracold collisions occurring in trapped gases. The properties of this treatment were further investigated in the context of the condensed Bose gases by Julienne and coworkers [15, 16] and by Blume and Greene [17]. These papers investigated the strong interactions that occur near a Feshbach resonance, and employed an energy-dependent scattering length to model this situation. Here we implement this model for a time-dependent magnetic field, augmented by the sudden approximation to model the rapid field ramps.

By performing a frequency rescaling, an initial condensate density can be achieved for two bodies that is comparable to the density range studied experimentally. The premise of our model is that the energy scale of the trap energy levels is very low in present day experiments, far smaller than the molecular binding energies of interest. At the same time, we anticipate that the physics of any single molecule formation is controlled by the interaction of just two atoms, even in a many-atom condensate. Accordingly, we consider just two atoms in an oscillator trap of very high frequency, adjusted so that the density of the two atoms becomes the same as the condensate density in the experiments. The resulting approach is then used to model the recent experimental results of Donley *et al.* [1]. Our two-body model is shown to describe most of the nontrivial features observed in the experiment, although some discrepancies remain. This may indicate that a more elaborate inclusion of the many-body effects may be necessary to achieve a full quantitative description. Nevertheless, our results show that more of the key effects can be interpreted in terms of two-body physics than appears to have been realized in existing theoretical models.

This paper is organized as follows: Section 2 determines the eigenstates of two trapped atoms using a quantum-defect-style method that differs from the treatment of Ref. [14] but is equivalent. Section 3 discusses the behavior of the atom pair close to a Feshbach resonance, and our approximate solution of the time-dependent Schrödinger equation using the sudden approximation. Section 4 discusses the frequency rescaling employed to interpret the many-atom system. Section 5 compares the results of our model with recent experiments, while Section 6 summarizes our conclusions.

2. Two Interacting Atoms in a Trap

We consider two atoms of mass m in a spherical oscillator trap of angular frequency ω , which interact through a zero-range potential $V(\mathbf{r})$ [18],

$$V(\mathbf{r}) = \frac{4\pi\hbar^2 a_{\text{sc}}}{m} \delta^{(3)}(\mathbf{r}) \frac{\partial}{\partial r} r. \quad (1)$$

Here a_{sc} is the two-body atom-atom scattering length and \mathbf{r} is the relative coordinate of the two particles. The Hamiltonian of the two-body system separates into a center of mass part and a relative part. The center of mass part has the usual harmonic oscillator solutions which are not affected by the scattering length; hence, we focus on the relative motion in the following.

Since the contact potential in Eq. (1) acts solely on the s -wave symmetry, we consider only solutions of the relative Schrödinger equation with zero orbital angular momentum. We define the harmonic oscillator length $a_{\text{ho}} = \sqrt{\hbar/(\omega m/2)}$ corresponding to the *reduced* mass, $m/2$, as our length scale, leading to a dimensionless radial coordinate $x = r/a_{\text{ho}}$. Our energy unit is chosen to be $\hbar\omega$, resulting in a dimensionless energy variable $\epsilon = E/\hbar\omega$. The s -wave eigenfunction $\phi_{\epsilon,l=0}$ of the radial Schrödinger equation in the relative coordinate corresponding to energy $\epsilon\hbar\omega$ is then rescaled,

$$\phi_{\epsilon,l=0} = \frac{u(x)}{x} \frac{1}{\sqrt{4\pi}}, \quad (2)$$

so that the radial equation has only second derivatives,

$$\left(-\frac{1}{2} \frac{d^2}{dx^2} + \frac{1}{2}x^2 \right) u(x) = \epsilon u(x). \quad (3)$$

The contact potential, Eq. (1), imposes a boundary condition on the logarithmic derivative of $u(x)$ at the origin:

$$\frac{u'(0)}{u(0)} = -\frac{a_{\text{ho}}}{a_{\text{sc}}}. \quad (4)$$

Solutions of these equations have been obtained by Busch *et al.* [14]. However, we now rederive these solutions in a slightly different manner, along the lines of quantum defect theory (QDT) [19].

We start with a pair of solutions of Eq. (3), f and g , that have regular,

$$f_{\nu}(x) = A_{\nu} x e^{-x^2/2} {}_1F_1(-\nu; \frac{3}{2}; x^2), \quad (5)$$

and irregular,

$$g_{\nu}(x) = B_{\nu} e^{-x^2/2} {}_1F_1(-\nu - \frac{1}{2}; \frac{1}{2}; x^2), \quad (6)$$

behavior at the origin, at any energy. Here ν denotes a quantum number, $\nu = \epsilon/2 - 3/4$, while A_{ν} and B_{ν} are constants that will be determined later. In the following, our solutions are characterized by the subscript ν instead of the subscript ϵ . We calculate the asymptotic behavior of the two solutions using the known behavior of the confluent hypergeometric function, ${}_1F_1$,

$${}_1F_1(a; b; x) \Big|_{x \rightarrow \infty} \rightarrow \frac{\Gamma(b)}{\Gamma(a)} x^{a-b} e^x + \cos(\pi a) \frac{\Gamma(b)}{\Gamma(b-a)} x^{-a}, \quad (7)$$

as well as the gamma reflection formula:

$$\Gamma(\nu) \Gamma(1 - \nu) = \frac{\pi}{\sin(\pi\nu)}. \quad (8)$$

For $x \rightarrow \infty$, we obtain

$$\begin{aligned} f_{\nu} &\rightarrow A_{\nu} \Gamma\left(\frac{3}{2}\right) \left(-x^{-2\nu-2} e^{x^2/2} \sin(\pi\nu) \frac{\Gamma(\nu+1)}{\pi} + x^{2\nu+1} e^{-x^2/2} \cos(\pi\nu) \frac{1}{\Gamma(\nu+\frac{3}{2})} \right), \\ g_{\nu} &\rightarrow B_{\nu} \Gamma\left(\frac{1}{2}\right) \left(-x^{-2\nu-2} e^{x^2/2} \cos(\pi\nu) \frac{\Gamma(\nu+\frac{3}{2})}{\pi} - x^{2\nu+1} e^{-x^2/2} \sin(\pi\nu) \frac{1}{\Gamma(\nu+1)} \right). \end{aligned}$$

Our goal is to recast these solutions in the “usual” QDT form [19] given by

$$f_\nu \rightarrow -C \left(D^{-1} e^{x^2/2} x^{-2\nu-2} \sin(\pi\nu) - D e^{-x^2/2} x^{2\nu+1} \cos(\pi\nu) \right), \quad (9)$$

$$g_\nu \rightarrow C \left(D^{-1} e^{x^2/2} x^{-2\nu-2} \cos(\pi\nu) - D e^{-x^2/2} x^{2\nu+1} \sin(\pi\nu) \right). \quad (10)$$

In addition, we want to normalize the functions f and g such that their Wronskian $W[f_\nu, g_\nu]$ is $2/\pi$. These requirements can be fulfilled by defining A_ν and B_ν [Eqs. (5) and (6), respectively] appropriately, which leads to

$$f_\nu = \frac{2}{\sqrt{\pi}} \sqrt{\frac{\Gamma(\nu + \frac{3}{2})}{\Gamma(\nu + 1)}} x e^{-x^2/2} {}_1F_1(-\nu; \frac{3}{2}; x^2), \quad (11)$$

$$g_\nu = -\frac{1}{\sqrt{\pi}} \sqrt{\frac{\Gamma(\nu + 1)}{\Gamma(\nu + \frac{3}{2})}} e^{-x^2/2} {}_1F_1(-\nu - \frac{1}{2}; \frac{1}{2}; x^2). \quad (12)$$

Using these normalizations, the constants C and D [Eqs. (9) and (10)] become $C = 1/\sqrt{\pi}$ and $D = \sqrt{\pi}/\sqrt{\Gamma(\nu + 1)\Gamma(\nu + 3/2)}$.

With these solutions for f and g in hand, we can proceed in the spirit of QDT by deriving a solution to the radial Schrödinger equation that accounts for an additional non-oscillator short-range potential. For distances beyond those where the short-range potential is non-negligible, the radial wave function u_ν must assume the form

$$u_\nu = f_\nu \cos \pi\mu - g_\nu \sin \pi\mu. \quad (13)$$

Armed with the known asymptotic behavior of f and g , we can determine the asymptotic behavior of u and impose the requirement that u is finite at large x (i.e., the coefficient of the growing exponential is zero). This leads to the equality $\sin \pi(\nu + \mu) = 0$, which can be recast as a quantization condition

$$\epsilon = 2(n - \mu) + \frac{3}{2}, \quad (14)$$

where $n = 0, 1, 2, \dots$. The last step towards finding the energy levels ϵ of our confined atom pair is to impose the boundary condition on the solution u , which is implied by the contact potential at the origin [Eq. (4)]. Using the fact that at small arguments ${}_1F_1(a; b; x)$ approaches 1 [20], we obtain

$$\frac{u'(0)}{u(0)} = -\frac{f'(0) \cos \pi\mu}{g(0) \sin \pi\mu} = -\frac{a_{\text{ho}}}{a_{\text{sc}}}. \quad (15)$$

Upon inserting the explicit forms for f and g as given in Eqs. (11) and (12), we obtain the following equation for the quantum defect μ (see also [17])

$$\tan \pi\mu = -\frac{a_{\text{sc}}}{a_{\text{ho}}} \frac{2\Gamma\left(\frac{\epsilon}{2} + \frac{3}{4}\right)}{\Gamma\left(\frac{\epsilon}{2} + \frac{1}{4}\right)}. \quad (16)$$

Equations (14) and (16) allow determination of the energy spectrum for any value of the scattering length a_{sc} . It can be shown that these equations are equivalent to the transcendental equation

$$\frac{2\Gamma\left(-\frac{\epsilon}{2} + \frac{3}{4}\right)}{\Gamma\left(-\frac{\epsilon}{2} + \frac{1}{4}\right)} = \frac{1}{a_{\text{sc}}/a_{\text{ho}}} \quad (17)$$

of Busch *et al.* [14]. The energy quantization conditions derived here for a zero-range pseudo potential using QDT also apply to a confined atom pair interacting through an arbitrary (i.e., non-contact) short-range potential, the only difference being that the quantum defect μ has a different value. Regardless of the specific short-range potential, the corresponding eigenfunctions u_ν are then given outside the potential range in terms of the hypergeometric U function [21, 14],

$$u_\nu(x) = N_\nu e^{-x^2/2} U\left(\frac{-(2\nu+1)}{2}, \frac{1}{2}, x^2\right),$$

where N_ν is a normalization constant.

3. Two atoms near a Feshbach Resonance. Overlap matrix elements

To apply our formalism derived above to two-atom states that lie energetically near a Feshbach resonance, we rewrite our scattering length a_{sc} as a function of the magnetic field strength B

$$a_{\text{sc}}(B) = a_{\text{bg}} \left(1 - \frac{\Delta}{B - B_0}\right).$$

Here, a_{bg} denotes the scattering length far from the resonance, B_0 denotes the resonance position, while Δ is a parameter related to the width of the resonance. In our numerical calculations (see Sec. 5), we choose parameter values in agreement with those obtained by fitting to recent experimental data [22] of the Feshbach resonance in ^{85}Rb : $B_0 = 155.041$ G, $\Delta = 10.71$ G, and $a_{\text{bg}} = -443$ a.u. Note that a similar model was employed in Ref. [16] for the case of a Feshbach resonance in ^{23}Na . While that study additionally incorporated an energy dependence of the scattering length, the energy dependence of $a_{\text{sc}}(B)$ in the present study is comparatively weak over the range of energies and magnetic fields considered. Hence we choose to neglect it.

Our goal is to describe our two-atom system when it is subjected to time-dependent magnetic field ramps $B(t)$, like the ones used in the experiments of [1]. To approximate the experimental $B(t)$, we assume a piecewise constant $B(t)$ as indicated in Fig. 3. In our approach the assumption of an instantaneous variation of $B(t)$ amounts to the use of the sudden approximation. In this approximation, the wavefunction of the atom pair is initially unaffected by the instantaneous change of $B(t)$. Let the magnetic field strength before (after) the instantaneous change be B_1 (B_2). It is then convenient to write the time-dependent superposition state Ψ at field strength B_1 in terms of the eigenfunctions $\{\phi_{\nu_1}\}_{\nu_1=0,\infty}$ (with corresponding eigenvalues $\{\epsilon_{\nu_1}\}_{\nu_1=0,\infty}$), and that at field strength B_2 in terms of the eigenfunctions $\{\phi_{\nu_2}\}_{\nu_2=0,\infty}$ (with corresponding eigenvalues $\{\epsilon_{\nu_2}\}_{\nu_2=0,\infty}$),

$$\Psi(B_j, t) = \sum_{\nu_j} a_{\nu_j}^{(j)}(t) \phi_{\nu_j}, \quad j = 1, 2. \quad (18)$$

The “new” expansion coefficients $a_{\nu_2}^{(2)}$ can be expressed through the “old” expansion coefficients,

$$a_{\nu_2}^{(2)} = \sum_{\nu_1} O_{\nu_2, \nu_1} a_{\nu_1}^{(1)},$$

where O_{ν_2, ν_1} denotes the overlap matrix between the eigenfunctions corresponding to B_1 and B_2 , respectively,

$$O_{\nu_2, \nu_1} = \langle \phi_{\nu_2} | \phi_{\nu_1} \rangle. \quad (19)$$

The following derivation shows how the eigenstate transformation projections O_{ν_2, ν_1} can be determined analytically. Let $u_{\nu_{1,2}}$ be the reduced radial wavefunctions corresponding to $\phi_{\nu_{1,2}}$. If we multiply the equation for u_{ν_1} by u_{ν_2} and that for u_{ν_2} by u_{ν_1} , subtract the resulting equations and integrate the result from 0 to ∞ , an integration by parts gives

$$(\epsilon_{\nu_1} - \epsilon_{\nu_2}) \int_0^\infty u_{\nu_1}(x) u_{\nu_2}(x) dx = W [u_{\nu_1}, u_{\nu_2}]_{x=0}. \quad (20)$$

Here, $W [u_{\nu_1}, u_{\nu_2}]_{x=0}$ denotes the Wronskian of u_{ν_1} and u_{ν_2} evaluated at the origin. The above formula allows the determination of both the normalization constant N_ν [Eq. (2)] and the overlap matrix element O_{ν_2, ν_1} [Eq. (19)],

$$O_{\nu_2, \nu_1} = N_{\nu_1} N_{\nu_2} \left[2 \cos(\pi \nu_1) \Gamma\left(\frac{3}{2} + \nu_1\right) \Gamma(1 + \nu_2) \sin(\pi \nu_2) \right. \\ \left. - 2 \cos(\pi \nu_2) \Gamma(1 + \nu_1) \Gamma\left(\frac{3}{2} + \nu_2\right) \sin(\pi \nu_1) \right] / [4 \pi (\nu_2 - \nu_1)] \quad (21)$$

and

$$N_\nu = \left\{ \Gamma(1 + \nu) \Gamma\left(\frac{3}{2} + \nu\right) \left[2\pi + \left(\psi(\nu) - \psi\left(\frac{1}{2} + \nu\right) \right) \sin(2\pi\nu) \right] \right\}^{-1/2}, \quad (22)$$

where ψ denotes the digamma function [20]. The overlap matrix elements O_{ν_2, ν_1} are expressed in terms of the ν quantum numbers, which, in turn, are directly linked to the energy eigenvalues ϵ through $\epsilon = 2\nu + 3/2$. Figure 1 shows examples of the dependence of the overlap matrix elements on the non-integer quantum numbers ν_1 and ν_2 . While the overlap matrix elements oscillate rapidly with $\Delta\nu$ ($\Delta\nu = \nu_2 - \nu_1$), our analytical formula for the matrix elements results in stable numerical calculations (see Sec. 5).

4. Description of many-body effects through a frequency rescaling

The simple model described in the previous section allows us to describe the states of a trapped atom pair that undergoes sudden changes of the interatomic interaction, here parameterized accurately through a magnetic field-dependent scattering length. Our goal is now to apply our two-atom model to interpret an ensemble of N atoms ($N \gg 2$). Without constructing a rigorous many-body approach like, e.g., the ones based on the field theory formalism, we will attempt to account for many-body effects by using our two-particle model with a rescaled frequency. The idea suggested by Cornell [23] is to capitalize on the importance of the diluteness or gas parameter $n a_{\text{sc}}^3$, (n is the density of atoms) which in more rigorous many-body models of degenerate Bose gases plays a key role in determining the behavior of the system. Instead of modeling an N -atom system we will model a two-body system that has the same diluteness parameter as the experimentally studied N atom sample.

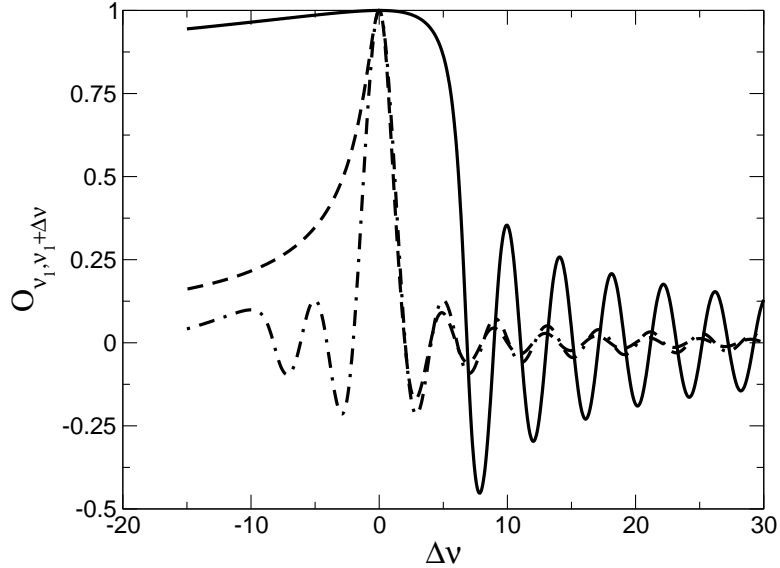


Figure 1. Dependence of the overlap matrix element O_{ν_2, ν_1} between two eigenfunctions corresponding to quantum numbers ν_1 and $\nu_2 = \nu_1 + \Delta\nu$ on the quantum number difference, $\Delta\nu$, for three values of ν_1 : $\nu_1 = -5$ (solid line), $\nu_1 = 1.5$ (dashed line), and $\nu_1 = 10$ (dashed-dotted line). Note that the solid line in this figure represents the projections of the molecular state onto the other trapped atom states.

To motivate that our two-body description can, at least to a crude level of approximation, account for many-body physics we calculate the overlap integral for one particular case. We consider the overlap integral between a two-body state located very far from the resonance centered at B_0 , $u_{\text{ho}}(r)$, with that corresponding to a value of B close to B_0 , $u_M(r)$. u_{ho} refers to the trap ground state, which we approximate through a state describing two independent atoms with zero scattering length,

$$u_{\text{ho}}(x) \approx \frac{2}{\pi^{1/4}} x e^{-x^2/2} \quad (23)$$

$u_M(r)$ denotes a molecular state (i.e., the state that remains bound even in the absence of the confining potential). Neglecting the influence of the confining potential we assume the wavefunction of this state to be:

$$u_M(r) \approx \sqrt{2\kappa} e^{-\kappa r}, \quad (24)$$

where $\kappa = 1/a_{\text{sc}}$. We estimate the overlap integral of these two states, by assuming that the exponential in u_{ho} is approximately 1 over the range relevant for the evaluation of the integral. This approximation yields

$$\langle u_M | u_{\text{ho}} \rangle \approx \left(\frac{2a_{\text{sc}}}{a_{\text{ho}}} \right)^{3/2} \pi^{-1/4}. \quad (25)$$

The absolute value of this overlap matrix element gives the probability p that the initially “unbound” atom pair ends up in the molecular state as the B field is tuned close to

resonance,

$$p = \frac{8}{\sqrt{\pi}} \left(\frac{a_{\text{sc}}}{a_{\text{ho}}} \right)^3. \quad (26)$$

For small p ($p \ll 1/N$), we can extend our two-body treatment to model an ensemble of N atoms. As the B field is tuned to resonance, *each atom pair* in the ensemble has the probability p to form a molecular bound state. Using this simple picture, the calculation of the fraction of atoms that transform into molecules, $f_{\text{atoms} \rightarrow \text{molecules}}$, due to the magnetic field ramp amounts to a simple counting of atom pairs,

$$f_{\text{atoms} \rightarrow \text{molecules}} = \frac{2}{N} \frac{N(N-1)}{2} p \approx Np = \frac{8}{\sqrt{\pi}} \frac{a_{\text{sc}}^3 N}{a_{\text{ho}}^3}. \quad (27)$$

Within our estimate, the fraction of atoms transformed to molecules is proportional to the diluteness parameter $n a_{\text{sc}}^3$ (the density is proportional to N/a_{ho}^3). This back-of-the-envelope estimate, although not a rigorous proof, provides a somewhat quantitative motivation for the idea that lies behind the frequency rescaling introduced above.

Since in our two body model we will choose a scattering length that is the same as in the sample used in the experiment, having the same diluteness parameter for the two amounts to having the same density. This condition, that our two atoms confined by the harmonic potential have the same peak density as the average many-body density, n , provides the criterion for determining our rescaled frequency ω' . For the purpose of evaluating ω' from this condition we neglect the atom-atom potential and consider the two non-interacting atoms in the ground state of the harmonic trap. Based on this assumption we find the relation between the density of the many-body sample, n , and the trap frequency confining the two atoms, ω' , to be

$$\omega' = \frac{\hbar}{m_{\text{atom}}} \pi \left(\frac{n}{2} \right)^{2/3}. \quad (28)$$

The experiment [1] uses an inhomogeneous trap that has a geometric mean of $\omega \approx 2\pi 12$ Hz, and involves approximately $N = 17100$ atoms. The starting value of the magnetic field of about 162.2 G corresponds to a scattering length of 220 a.u.. For these parameters, using either the Thomas-Fermi formula or the Gross-Pitaevskii equation, one obtains a density profile with an average of approximately $n \approx 4 \cdot 10^{12} \text{ cm}^{-3}$ (see, e.g., Fig. 10 of Ref. [9]). Note that this is lower than the claimed experimental density of $n = 1.1 \cdot 10^{13} \text{ cm}^{-3}$. We find that the final results (see Fig. 4) depend sensitively on density, and this way of rescaling the frequency in Eq. (28) seems to best reproduce the experimental results. The rescaled frequency that we obtain for this density ($n = 4 \cdot 10^{12} \text{ cm}^{-3}$) is $\omega' \approx 2\pi 3.72$ kHz.

Figure 2 shows the eigenvalues of two ^{85}Rb atoms confined by a harmonic potential with angular frequency ω' as a function of the magnetic field strength B in the vicinity of the Feshbach resonance described through the parameters given in Sec. 3. Notice that the sequence of avoided crossings of energy levels associated with the Feshbach resonance becomes smeared out at this high frequency. We group the two-body states into three groups (see Fig. 2): the molecular state, the trap ground state, and the

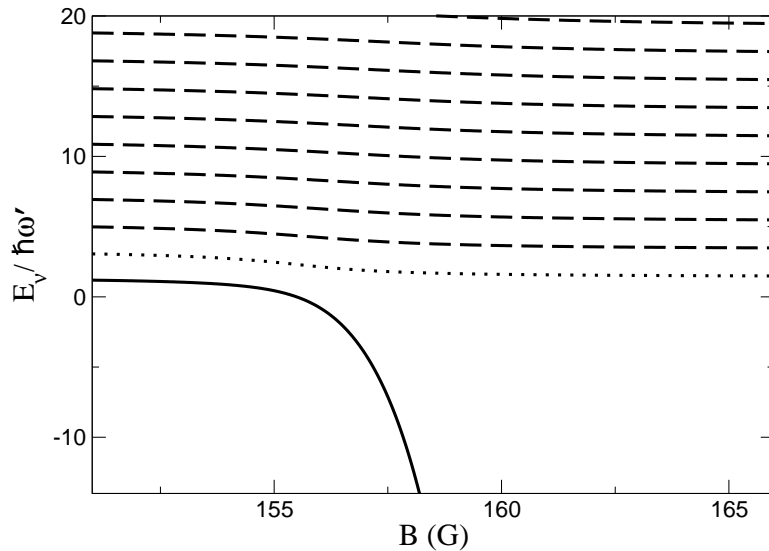


Figure 2. Energy eigenvalues for two ^{85}Rb atoms for a rescaled frequency $\omega' = 2\pi 3.72$ kHz (corresponding to $N = 17100$) near a Feshbach resonance centered at $B_0 = 155.041$ G with $a_{\text{bg}} = -443$ a.u. and $\Delta = 10.71$ G. We distinguish three groups of states: the molecular state (solid line), the trap ground state (dotted line), and the trap excited states (dashed lines).

excited states of the trap. To connect our two-body study to the N -body systems studied experimentally, we make the following correspondence between the two-atom states and the many body states. The molecular state of two atoms is in the ground state of the center-of-mass motion, and accordingly we associate this population with translationally cool (condensed) molecules in the N -atom system. At fields above the resonance, the lowest *positive* energy state (which we refer to as the trap ground state) corresponds to condensate atoms. Finally, the higher trap excited states correspond to non-condensed atoms, i.e., the experimentally observed “jets of hot atoms” [1]. In the next section, we interpret the occupation probability of the two-atom states as the fraction of atoms ending up in the corresponding many body states.

5. Numerical Results

We now use the above description to simulate the experiment of Donley *et al.* [1]. This experiment consists of applying two magnetic field pulses, separated by a time interval of variable length (denoted by t_{evolve} in Fig. 3), to a condensed sample of ^{85}Rb atoms. The two pulses of durations t_1 and t_2 , respectively, ramp the magnetic field to B_m , a value close to the Feshbach resonance, which couples the atomic and molecular states of the sample. After the application of these magnetic pulses, three distinct components are identified experimentally: a remaining sample of condensed atoms, a

hot burst of atoms, and a “missing” component which is not detected under the current experimental conditions. At least two theoretical approaches [8, 9], both involving a field theory formalism, identified this third component (i.e., the missing component) as a molecular condensate, however, other interpretations exist. The size of the three components oscillates as a function of the evolve time t_{evolve} with a frequency that corresponds to the energy of a weakly-bound, vibrationally excited state of the $^{85}\text{Rb}_2$ dimer.

We model the experimental situation using the sudden approximation to describe the sharp rises and drops of the magnetic field. At time $t = 0$ in Fig. 3, our initial state is chosen to be the trap ground state corresponding to the initial value of the magnetic field, B_i . This initial state is then propagated in time. During the time period where the magnetic field is unchanged, $B(t) = B_i$, the time propagation simply modulates the phase of the initial state. After the magnetic field changes to the value $B(t) = B_m$, the system is projected onto the new eigenstates at that field. We then propagate the quantum amplitudes of the two-atom energy eigenstates. At the end of the double pulse, when the magnetic field becomes B_f , our final state is expanded in the ϕ_ν states corresponding to the final value of the magnetic field, B_f . Using the correspondence between two-body and many-body states discussed in the previous section, we then relate the final population probabilities to the Donley *et al.* experiment. In taking the absolute square of this final quantum amplitude for each distinguishable final state, cross terms arise that exhibit quantum beats, the most prominent of which is between the molecular state and the atomic trap ground state (condensate). The parameters entering our simulations are the rescaled frequency ω' , the four magnetic field values B_i , B_{evolve} , B_m and B_f , as well as the three time periods t_1 , t_{evolve} and t_2 . Our particular simulation values are given in the caption of Fig. 3.

Figure 4 shows the results of our time-dependent two-atom calculation for a scaled frequency ω' that gives a two-atom density of $4 \cdot 10^{12} \text{ cm}^{-3}$. This figure can be directly compared with Fig. 6 of Ref. [1]. Inspection of these two figures shows reasonable agreement in the average values and the oscillation amplitudes for the three components. In addition, our results reproduce approximately the relative phases of the oscillations of the three different populations. The observed agreement is remarkable if one considers that we have used the sudden approximation for magnetic field ramps that in the experimental conditions last about $15 \mu\text{s}$. We have also assumed that the atomic sample has a constant (average) density across the atom cloud, while an improved model could consider averaging over a distribution of densities (see, for example, [8]). The frequency of the beats that we observe is approximately 150 kHz in accordance with the bound state energy produced by our parametrization of the scattering length given in Eq. (3). In contrast, the experiment measures oscillations at approximately 196 kHz for the same value of B_{evolve} . In fact, a possible way to improve our model would be to use a better description of the atom-atom scattering properties, and consequently, a more accurate value of the molecular binding energy. Our estimations show that inclusion of the energy dependence up to the effective range level (the first non-zero correction, see

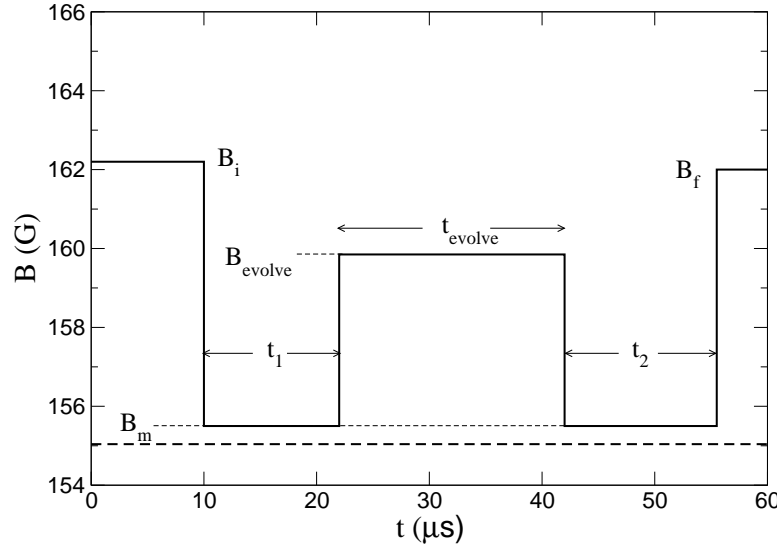


Figure 3. Magnetic field B as function of time t in our modeling of the experiments of Donley *et al.*. The thick dashed line represents the position of the Feshbach resonance, $B_0 = 155.041\text{G}$. The abrupt variations of the magnetic field reflect our use of the sudden approximation. The parameters of the pulse are: $B_i = 162.2\text{ G}$, $B_m = 155.5\text{ G}$, $B_{\text{evolve}} = 159.85\text{ G}$, $B_f = 162\text{ G}$, and $t_1 = 12\text{ }\mu\text{s}$, $t_2 = 13.6\text{ }\mu\text{s}$.

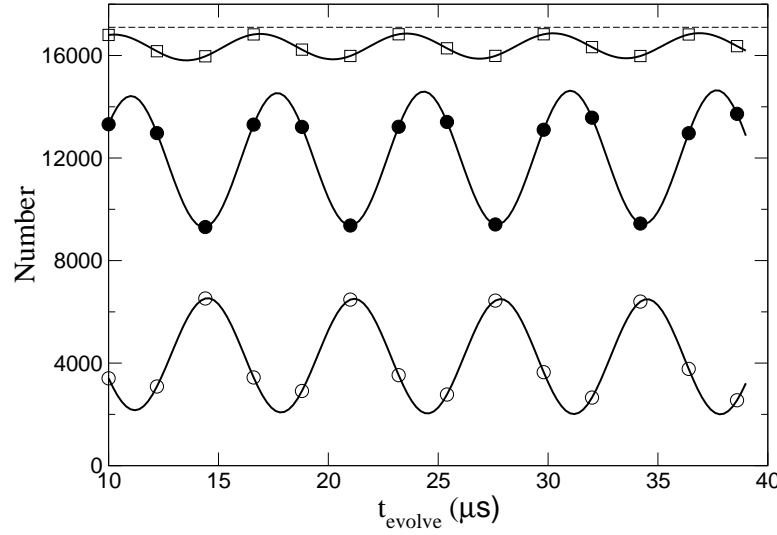


Figure 4. Population of the ground trap state (filled circles) and of the excited trap states (open circles) at the end of the magnetic field pulse shown in Fig. 4. The sum of the two populations is plotted with squares and allows determination of the number of atoms that made the transition to molecules by subtraction from the total number of atoms ($N = 17100$).

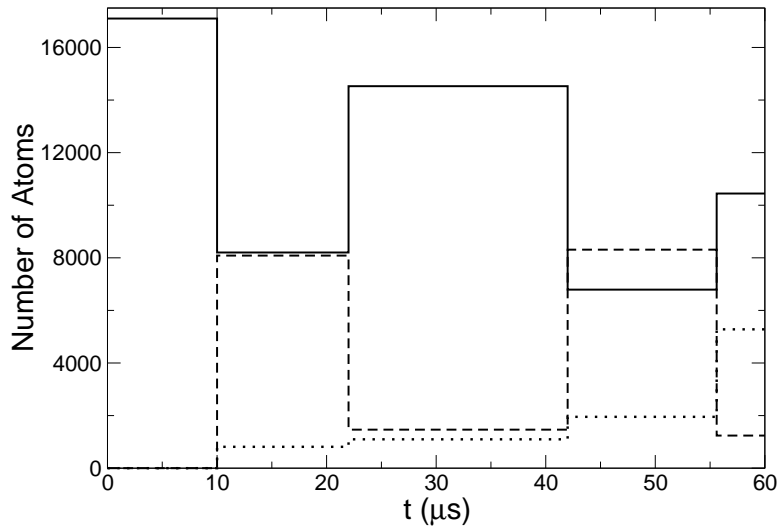


Figure 5. Evolution of population of the three types of states as a function of time during one magnetic field double-pulse (with $t_{\text{evolve}} = 20 \mu\text{s}$, identical to the one plotted in Fig. 3). Solid line: trap ground state population (condensate); dashed line: molecular state population; dotted line: population of the excited trap states (“burst” atoms).

[17]) significantly improves the agreement between the bound state energy produced by our simple model and by a multichannel calculation. However, in order to maintain our simple description of the system dynamics during the pulse evolution, we do not include this correction here.

Note that our rescaled frequency yields $\hbar\omega'/k_B \approx 180 \text{ nK}$, which implies that the first excited pair above the trap ground state would share approximately two times this energy. We note that the resulting energy per atom for the least energetic of our “hot atoms” is approximately 180 nK above the trap ground state. This is not very far from the experimentaly observed energy (150 nK) of the burst atoms. However, including all excited trap states, our model predicts that burst atoms will have a higher average energy than in the experiment. In addition, our model predicts a dependence of the energy of the hot atoms on the initial atomic density like the one given by Eq. (28) while the experiment does not mention an observable density dependence of the energy of the hot bursts. We conclude that the rescaling used in our model allows a reasonable prediction of the number of the hot atoms, but has a limited ability to account for their energy distribution.

Figure 5 shows the evolution of the populations during only one pulse (with $t_{\text{evolve}} = 20 \mu\text{s}$) as a function of time. According to our calculations, the molecular eigenstate and the excited states (i.e., the non-condensed atoms) acquire roughly comparable populations after the complete first pulse (after $t = 22 \mu\text{s}$) and mantain them until the last ramp of the pulse, when the population of the excited states becomes

considerably larger. The significant population we observe for the molecular state during t_{evolve} supports our interpretation of the quantum beats seen in the end-of-pulse populations. These beats are the result of the interference of quantum paths that go through the intermediate molecular state with those that go through the intermediate ground or excited trap states. (The difference between the latter is too small to show up on the time scales considered here.) The predictions of this two-atom model, concerning the intermediate time populations of the molecular and hot components, are consistent with the comments of Braaten *et al.*, [10] (see also [24]) which point out the difficulty of interpreting the intermediate populations shown in Ref. [8]. Interpretation of the results of Kokkelmans and Holland [8] is complicated by the fact that their two-body representation does not consist of eigenfunctions of the molecular Hamiltonian. Accordingly, their "molecular state" is not actually the two-body molecular eigenstate, except at magnetic fields well above 160 G. In problems with a linear Schrödinger equation, a simple basis change could always be carried out, to re-express the physics in an eigenrepresentation. Here, however, the nonlinearity of the coupled equations complicates this transformation. At the same time, as Braaten *et al.* [10] comment, the success of the final calculations in reproducing the experimental observations with no adjustable parameters is immediately apparent and convincing that the right two-body physics has been incorporated into the formulation. We mainly recommend caution in interpreting the meaning of the "molecular state" in the Kokkelmans and Holland formulation, except at high magnetic fields where it approximately coincides with a two-body eigenstate.

The two-atom model disagrees with a specific qualitative prediction of Mackie *et al.* [11]. Whereas in our model the "hot" atoms at the end of the pulse can be created through any of the three intermediate states (i.e, molecules, condensed atoms or non-condensed atoms), in the model of Ref. [11] the "hot" atoms are solely the results of the "rogue dissociation" of intermediate molecular states. Our approach suggests that around half of the final hot atoms are not produced by rogue dissociation. In fact, the pathway *condensate* \rightarrow *hot atoms*, which is apparently neglected by Ref. [11], is of comparable importance. This may in fact be the additional loss mechanism that is cited as being "missing" in Ref. [11].

6. Conclusions

We have investigated the results given by a simple model of the dynamics of two trapped atoms near a Feshbach resonance. Our model accounts for the interaction between the two atoms using a zero range potential and it also includes the confinement of the atoms by an external harmonic trap. This model can be used to make predictions regarding atomic Bose condensate driven with the help of magnetic fields near a Feshbach resonance, if a rescaled frequency is used to achieve a density comparable to the density of the many-atom condensates studied experimentally. A correspondence can be drawn between the three components observed in the recent field-ramp experiments and

three groups of two-body states in our model. The experimentally-observed burst of hot atoms appears in our model as atom pairs excited to states energetically higher than the trap ground state level. The two-atom model is able to predict the populations of these three states, in fair agreement with the experimental observations. Accordingly this may provide a useful alternative view of the physics of coherent atom-molecule coupling in a condensate. The success of a two-body description may initially seem surprising, because the dominant physical processes occurring in condensate experiments near a Feshbach resonance are normally viewed as being inherently many-body in nature. Nevertheless, the present study suggests that a two-body picture, with minimal modifications, is sufficiently realistic to be used for simple estimates at a qualitative or semiquantitative level.

Acknowledgments

We thank E. Cornell for helpful suggestions and encouragement. We also thank N. Claussen, J. Dunn, M. Holland, and C. Wieman for informative discussions. This work was supported by NSF.

References

- [1] Donley E A, Claussen N R, Thompson S T and Wieman C E 2002 *Nature* **417** 529
- [2] Zoller P 2002 *Nature* **417** 493
- [3] Heinzen D J, Wynar R, Drummond P D and Kheruntsyan K V 2000 *Phys. Rev. Lett.* **84** 5029
- [4] Inouye S, Andrews M R, Stenger J, Miesner H -J, Stamper-Kurn D M and Ketterle W 1998 *Nature* **392** 151
- [5] Cornish S L, Claussen N R, Roberts J L, Cornell E A and Wieman C E 2000 *Phys. Rev. Lett.* **85** 1795
- [6] Timmermans E, Tommasini P, Côté R, Hussein M and Kerman A 1999 *Phys. Rev. Lett.* **83** 2691
- [7] Claussen N R, Donley E A, Thompson S T and Wieman C E 2002 *Phys. Rev. Lett.* **89** 010401
- [8] Kokkelmans S J J M F and Holland M J 2002 *Phys. Rev. Lett.* **89** 180401
- [9] Köhler T, Gasenzer T and Burnett K 2003 *Phys. Rev. A* **67** 013601
- [10] Braaten E, Hammer H W, Kusunoki M 2003 Comment on “Ramsey Fringes in a Bose-Einstein Condensate between Atoms and Molecules” *Preprint cond-mat/0301489*
- [11] Mackie M, Suominen K -A and Javanainen J 2002 *Phys. Rev. Lett.* **89** 18403
- [12] Duine R A and Stoof H T C 2003 *cond-mat/0302304*
- [13] Andrä H J 1970 *Phys. Rev. Lett.* **25** 325
- [14] Busch T, Englert B -G, Rzäżewski K and Wilkens M 1997 *Found. Phys.* **28** 549
- [15] Tiesinga E, Williams C J, Mies F H and Julienne P S 2000 *PR A* **61** 063416
- [16] Bolda E L, Tiesinga E and Julienne P S 2002 *Phys. Rev. A* **66** 013403
- [17] Blume D and Greene C H 2002 *Phys. Rev. A* **65** 043613
- [18] Demkov Yu N and Ostrovskii V N 1988 *Zero-range Potentials and their Applications in Atomic Physics* (Plenum Press, New York)
- [19] Greene C, Fano U and Strinati G 1979 *Phys. Rev. A* **19** 1485
- [20] Abramowitz M and Stegun I A 1970 *Handbook of Mathematical Functions* (New York: Dover Publications, Inc.) p. 504
- [21] See eq. 13.1.3 of Ref. [20]

- [22] Claussen N R, Kokkelmans S J J M F, Thompson S T, Donley E A and Wieman C E 2003
cond-mat/0302195
- [23] Cornell E A *private communication*
- [24] Duine R A and Stoof H T C 2003 *cond-mat/0211514*